Published in final edited form as:
Neuron. 2011 April 14; 70(1): 51–65. doi:10.1016/j.neuron.2011.02.039.

A RasGRP, *C. elegans* RGEF-1b, Couples External Stimuli to Behavior by Activating LET-60 (Ras) in Sensory Neurons

Lu Chen, **Ya Fu**, **Min Ren**, **Bing Xiao**, and **Charles S. Rubin**
Department of Molecular Pharmacology, Atran Laboratories, Albert Einstein College of Medicine, Bronx, NY, 10461

SUMMARY

RasGRPs, which load GTP onto Ras and Rap1, are expressed in vertebrate and invertebrate neurons. Functions, regulation and mechanisms of action of neuronal RasGRPs are unknown. Here, we show how *C. elegans* RGEF-1b, a prototypical neuronal RasGRP, regulates a critical behavior. Chemotaxis to volatile odorants was disrupted in RGEF-1b deficient (*rgef-1* null) animals and wild type animals expressing dominant negative RGEF-1b in AWC sensory neurons. AWC-specific expression of RGEF-1b-GFP restored chemotaxis in *rgef-1* null mutants. Signals disseminated by RGEF-1b in AWC neurons activated a LET-60(Ras)-MPK-1(ERK) signaling cascade. Other RGEF-1b and LET-60 effectors were dispensable for chemotaxis. A bifunctional C1 domain controlled intracellular targeting and catalytic activity of RGEF-1b and was essential for sensory signaling in vivo. Chemotaxis was unaffected when Ca^{2+}-binding EF hands and a conserved phosphorylation site of RGEF-1b were inactivated. Diacylglycerol-activated RGEF-1b links external stimuli (odorants) to behavior (chemotaxis) by activating the LET-60-MPK-1 pathway in specific neurons.

INTRODUCTION

The p21 GTP binding protein Ras functions as a molecular switch (Buday and Downward, 2008). Ras-GDP is inactive, but exchange of GTP for GDP induces conformational changes that enable Ras to activate effectors. Signals disseminated by Ras regulate cell proliferation and differentiation. Ras also mediates signaling in non-dividing, terminally differentiated cells, such as neurons. The Ras-ERK pathway is essential for optimal synaptic transmission, synaptic plasticity and the creation of certain types of memory (Thomas and Huganir, 2004). Mutations in proteins comprising the Ras-ERK and Ras-phosphatidylinositol 3-kinase (PI3K) signaling cascades cause human learning deficiencies and mental retardation (Krab et al., 2008).

Mechanisms governing Ras activation in adult neurons are poorly understood. Several GTP/GDP exchange factors (GEFs) catalyze Ras activation (Bos et al., 2007; Buday and Downward, 2008). SOS is an abundant Ras activator in embryonic and post-natal neurons. However, SOS protein declines at puberty and its GTP exchange capacity is low in adult neurons (Tian et al., 2004). RasGRF1, a Ca^{2+}-calmodulin activated GEF, associates with dendritic plasma membrane in mature neurons and promotes Ras activation at certain post-synaptic sites. Little is known about GEFs that control pre-synaptic Ras activation or

calmodulin independent, post-synaptic Ras-ERK signaling. Ras guanine nucleotide releasing proteins (RasGRPs) are candidates to fulfill these roles.

Four genes encode mammalian RasGRPs, which load GTP onto Ras and Rap1 (Buday and Downward, 2008; Stone, 2006). The GEFs are expressed in platelets, T-cells, B-cells and mast cells, where they regulate clotting, positive T-cell selection and differentiation, IgG production and inflammation. RasGRPs accumulate in many types of neurons (Toki et al., 2001), but functions of neuronal RasGRPs are unknown.

RasGRPs contain a predicted diacylglycerol (DAG)/phorbol 12-myristate-13-acetate (PMA)-binding C1 domain, two putative Ca^{2+}-binding EF hands, a conserved protein kinase C (PKC) phosphorylation site and a CDC25-related catalytic domain (Stone, 2006). PMA, DAG, Ca^{2+} and phosphorylation stimulate RasGRP activity in cultured cells. Thus, RasGRPs may integrate signals generated by multiple stimuli. Activation of RasGRP by DAG can trigger signaling that bypasses DAG-regulated PKCs. This expands the range of cell functions controlled by DAG and places Ras effectors under control of hormones and neurotransmitters (NTs) that activate phospholipase C (PLC) β, γ and ε. PLCs produce DAG and inositol 3, 4, 5-trisphosphate (IP3) by hydrolyzing phosphatidylinositol 4, 5-bisphosphate ($PI4,5P_2$). IP3 binds a receptor/channel in endoplasmic reticulum (ER), thereby eliciting Ca^{2+} efflux into cytoplasm. DAG enhances NT and neuropeptide (NP) release during synaptic transmission in mammalian and *C. elegans* nervous systems (de Jong and Verhage, 2009; Lackner et al., 1999; Sieburth et al., 2007). A logical hypothesis is that neuronal RasGRPs couple signals carried by DAG and Ca^{2+} to regulation of synaptic transmission by activating Ras.

An important caveat is that evidence supporting a current model for RasGRP regulation is limited. Control of RasGRP translocation or activity by the C1 domain is inferred from properties of mutant proteins lacking the entire domain (Caloca et al., 2003; Tognon et al., 1998). Loss of catalytic activity due to deletion-induced mis-folding is not excluded. The idea that EF hand motifs regulate RasGRPs by binding Ca^{2+} is unverified (Tazmini et al., 2009). Phosphorylation of RasGRP3 by DAG-activated PKC optimizes GTP exchange activity (Zheng et al., 2005). However, non-phosphorylated RasGRP3 promoted Ras and ERK activation in transfected cells; and pan-PKC inhibitors did not alter RasGRP3 phosphorylation or activity when DAG was increased by activating B-cell receptors (Teixeira et al., 2003; Zheng et al., 2005). Regulation of RasGRP by the C1 domain, EF hands and phosphorylation requires clarification.

RasGRP genes were disrupted (Coughlin et al., 2006), but neuronal functions of the GTP exchangers remain undiscovered. This may be due to functional redundancies among multiple Ras GEFs. Central questions regarding neuronal RasGRPs follow: Are RasGRPs prominent regulators of Ras or Rap1 signaling in normal neurons? What functions are placed under DAG/Ca^{2+} control by RasGRPs? Are RasGRPs indispensable regulators of neuronal physiology? Are RasGRPs essential in specific neurons or required throughout circuits? Is RasGRP catalytic activity regulated by DAG, Ca^{2+} and phosphorylation in vivo? Does neuronal RasGRP differentially activate Ras, Rap, ERK, PI3K or other effectors?

The preceding problems and questions were addressed by using *C. elegans* for incisive in vivo analysis. *C. elegans* is readily manipulated by molecular genetics, gene disruption and transgenesis; and its' neuronal physiology, nervous system circuitry and behavior are regulated by signaling molecules, pathways and mechanisms that are conserved in mammals (Bargmann, 2006). Here, we characterize *C. elegans* RGEF-1b, a neuronal RasGRP. A null mutation in the *rgef-1* gene disrupted chemotaxis to volatile odorants. Expression of RGEF-1b-GFP in AWC neurons restored chemotaxis in mutant animals. Conversely,

accumulation of dominant negative RGEF-1b^{R290A}-GFP in AWC neurons suppressed chemotaxis in wild type (WT) animals. Thus, RGEF-1b is indispensable for odorant-induced signal transduction and regulation of downstream circuitry. LET-60 (Ras) was identified as a critical RGEF-1b substrate-effector in AWC neurons. Signals disseminated by RGEF-1b triggered activation of the LET-60-MPK-1 (Ras–ERK) signaling cascade in AWC neurons. Other RGEF-1b effectors, including RAP-1, SOS-1 and AGE-1 (PI3K), were non-essential for chemotaxis. EGL-30, EGL-8 and DAG were characterized as major RGEF-1b regulators in AWC neurons. By avidly binding PMA or DAG, a bifunctional C1 domain mediated both intracellular targeting and activation of RGEF-1b. Elimination of catalytic activity or a moderate reduction in DAG binding affinity of the C1 domain disrupted RGEF-1b function in vivo. Chemotaxis was unaffected by mutations that inactivated Ca^{2+}-binding EF hands or a conserved PKC phosphorylation site. Thus, RGEF-1b links external stimuli (odorants) and internal DAG to the control of behavior (chemotaxis) by differentially activating the LET-60-MPK-1 cascade in AWC neurons.

RESULTS

Discovery and properties of RGEF-1b

A single gene, named *rgef-1* (Ras GTP/GDP exchange factor-1), was identified by searching *C. elegans* genome, EST and protein databases for RasGRP homologs. Cosmid F25B3 (GenBank) contains the *rgef-1* gene (4893 bp) and flanking DNA. RGEF-1 cDNA and protein were not previously characterized. Thus, RGEF-1 cDNAs were amplified by RT-PCR and cloned into a mammalian expression vector pCDNA3.1 (see Supplemental Experimental Procedures). Sequencing revealed that alternative splicing generated two cDNAs as diagrammed in Fig. S1A. RGEF-1a and RGEF-1b (Fig. S1E) cDNAs encode proteins composed of 654 and 620 amino acids, respectively (Fig. S1B). The isoforms are 98% identical and diverge only in a segment of unknown function that links a C1 domain to the C-terminal region. Quantitative real time PCR (qR-PCR) analysis disclosed that RGEF-1b mRNA accounts for >95% of *rgef-1* gene transcripts (Fig. S1C). Thus, studies were focused on RGEF-1b.

The predicted RGEF-1b protein (M_r ~ 70,000) contains structural (REM), catalytic (GEF) and regulatory (two EF hands and C1) domains that share substantial amino acid sequence identity and similarity with corresponding domains in human RasGRPs (Fig. S1D). By analogy, the RGEF-1b GEF domain will promote opening of the GTP/GDP binding site in small G-proteins (Bos et al., 2007). Guanine nucleotides will equilibrate between G-protein and cytoplasm. Since the GTP:GDP ratio is ~10, the net result is exchange of GTP for GDP. EF-hands, which contain 5 Asp or Glu residues, often regulate enzymatic activity by binding Ca^{2+} (Gifford et al., 2007). The C1 domain is predicted to mediate RGEF-1b translocation by binding membrane associated DAG (Hurley and Misra, 2000). Functions of RasGRP REM domains are unknown. Locations of domains along the RGEF-1b and RasGRP polypeptides are also preserved (Fig. S1D). RGEF-1b translocates to membranes and catalyzes loading of GTP onto LET-60 Ras in PMA-treated cells (see below). Together, these properties show that RGEF-1b is a new, but prototypical RasGRP.

RGEF-1b catalyzes GTP exchange on LET-60 Ras and RAP-1

In *C. elegans*, unique genes encode a 21 kDa Ras homolog (LET-60) and a 21 kDa Rap1 polypeptide (RAP-1). LET-60 and RAP-1 cDNAs were inserted into a modified pCDNA3.1 plasmid that appends an N-terminal Flag epitope tag to encoded proteins. If RGEF-1b is a RasGRP, it will translocate to membranes and mediate loading of GTP onto co-localized LET-60 or RAP-1. Because translocation of RasGRPs and substrates is not accurately replicated in vitro, assays were performed with intact cells.

Cells were co-transfected with RGEF-1b and either FLAG-tagged LET-60 or RAP-1 transgenes. After incubation with 50 nM PMA or vehicle for 15 min, cells were lysed and amounts of LET-60-GTP or RAP-1-GTP were assayed by Western immunoblot analysis. RGEF-1b promoted modest accumulation of LET-60-GTP in untreated cells (Fig. 1A, lane 3). In contrast, RGEF-1b activity increased ~6-fold when cells were incubated with PMA (Fig. 1A, lane 4).

If RGEF-1b has a functional C1 domain, it will be regulated by endogenous DAG. Cells were transfected with bombesin receptor, RGEF-1b and FLAG-LET-60 transgenes. Bombesin receptor, which has 7 transmembrane domains and couples with heterotrimeric Gq protein, promotes DAG production (Feng et al., 2007). When bombesin peptide binds, the receptor elicits PLCβ activation via Gαq-GTP. PLCβ generates DAG and IP3 by cleaving $PI4,5P_2$ in membranes. Incubation of cells with bombesin increased RGEF-1b mediated LET-60 activation ~4-fold (Fig. 1B, lanes 3 and 4). Stimulation by both bombesin and PMA (a DAG surrogate) suggests that DAG is a major regulator of RGEF-1b catalytic activity.

Modest basal and PMA-stimulated accumulation of RAP-1-GTP was evident in HEK293 cells lacking RGEF-1b because of endogenous GEFs (Fig. 2C, lanes 1 and 2). Expression of RGEF-1b elicited increased accumulation of RAP-1-GTP in the absence of stimuli (Fig. 1C, lane 3). Moreover, PMA further enhanced RGEF-1b catalyzed loading of GTP onto RAP-1 (Fig. 1C, lane 4). Thus, LET-60 and RAP-1 are RGEF-1b substrates.

The *rgef-1* gene promoter is active in neurons

A fragment of genomic DNA (2670 bp) that precedes exon 1 of the *rgef-1* gene was amplified by PCR. This DNA, which contains promoter-enhancer elements, was inserted upstream from a green fluorescent protein (GFP) reporter gene in a *C. elegans* expression plasmid (pPD 95.77). Animals stably expressing the *rgef-1*::GFP transgene were generated by microinjection. Cells producing GFP were identified by fluorescence microscopy and reference to the WORMATLAS anatomy database. *rgef-1* promoter activity was evident in a high proportion of neurons (Fig. 2, A and C) in 4 independently isolated strains. GFP was not detected in non-neuronal cells. Terminal divisions and differentiation of neurons were completed before *rgef-1* promoter activity was switched on during late embryonic development (Fig. 2E). Pan-neuronal GFP fluorescence was sustained from the end of embryogenesis (hatching) through adulthood.

RGEF-1b is essential for a critical behavior: chemotaxis to volatile odorants

We characterized a gene deletion mutant *(rgef-1(ok675)*) acquired from the *C. elegans* Knockout Consortium. Gene fragments were amplified by PCR (Fig. S2). DNA sequencing revealed that nucleotides 1493–2594 were deleted from the *rgef-1* gene. This eliminated exons 5–7 and part of exon 8 (Figs. S1A and S2), which encode the RGEF-1b catalytic domain. Splicing of exon 4 to exon 9 would yield a mutant protein lacking GTP exchange activity. Thus, the disrupted *rgef-1* gene is a null mutant. The mutant allele is designated *rgef-1(−/−)* or *rgef-1* null below.

RGEF-1b deficiency did not alter viability or fertility, or elicit obvious developmental defects. Thus, *rgef-1(−/−)* animals were exposed to volatile odorants, which simulate beneficial nutrients and induce chemotaxis. Volatile attractants, benzaldehyde (BZ), isoamyl alcohol (IAA) and 2-butanone (BU) are detected by a pair of AWC sensory neurons; AWA neurons detect diacetyl (Bargmann et al., 1993). Outputs from AWC and AWA regulate neuronal circuits underlying chemotaxis. *C. elegans'* responses to odorants were quantified by measuring chemotaxis index (CI) values (Experimental Procedures). High CI values

verified that WT *C. elegans* was strongly attracted to odorants (Fig. 3A). In contrast, behavior of RGEF-1b deficient animals was markedly defective. Chemotaxis to IAA, diacetyl, BZ and BU was suppressed ~ 10-, 4-, 4- and 3-fold, respectively (Fig. 3A). Assays can be compromised if mutants have movement defects. However, RGEF-1b depleted and WT *C. elegans* had similar abilities for coordinated movement in a standard locomotion assay (Fig. 3B). Thus, RGEF-1b depletion disrupts odorant-induced chemotaxis.

rgef-1(−/−) animals were reconstituted with an *rgef-1*::RGEF-1b-GFP transgene. RGEF-1b-GFP and unmodified REGF-1b had similar basal and PMA-stimulated GTP loading activities in HEK293 cells (Fig. 3C). *rgef-1* promoter-enhancer DNA ensured neuronal expression of RGEF-1b-GFP during appropriate developmental stages. Biosynthesis of REGF-1b-GFP in *rgef-1(−/−)* animals restored WT CI values for odorants (Fig. 3A). Loss of RGEF-1b function was established as the molecular basis for defective chemotaxis.

The possibility that RGEF-1b deficiency caused subtle developmental changes in the nervous system was explored. RGEF-1b cDNA was placed under regulation of a heat shock promoter (*hsp-16.2*) in expression vector pPD 95.77. The promoter is inactive at 20°C, but is activated in somatic cells when the temperature is raised to 32°C. Temperature-dependent induction of an *hsp-16.2*::RGEF-1b-GFP transgene for 60 min reconstituted AWC-dependent chemotaxis in adult *rgef-1(−/−)* animals that progressed through all developmental stages in the absence of RGEF-1b protein (Fig. 3D). Thus, RGEF-1b is not involved in development. Rather, the GTP exchanger is essential for transducing signals generated when *C. elegans* encounters attractive odors.

RGEF-1b deficient animals detect odorants

Prolonged exposure to attractive odorant in the absence of food can elicit a behavioral change in *C. elegans*. After washing, treated animals avoid the conditioning odorant, yielding negative CI values. WT and RGEF-1b depleted animals exhibited similar, negative CI values after preincubation with BU or BZ (Figs. S3A, S3B). Thus, the behavioral switch to odor avoidance was preserved in animals lacking RGEF-1b. Detection of odorant is a pre-requisite for the switch from attraction to aversion. Thus, the ODR-3-TAX-2/TAX-4 signaling pathway, which mediates odor detection by AWC cilia, (Bargmann, 2006), is operative in *rgef-1* null animals.

Expression of RGEF-1b in AWC neurons rescues chemotaxis

Neuronal circuitry underlying attraction to BZ, BU and IAA includes AWC sensory neurons and ~20 interneurons and motor neurons. Thus, expression of RGEF-1b-GFP in a few neurons might restore chemotaxis in *rgef-1(−/−)* animals. Three promoters were used to drive RGEF-1b-GFP expression. The *odr-1* promoter is active in AWC, AWB and I1 neurons; *odr-3* drives transcription in AWA, AWB, AWC and 4 other neurons; and the *gpa-3* promoter is silent in chemosensory neurons, but active in a dozen distinct neurons (L'Etoile and Bargmann, 2000; Lans et al., 2004). An *odr-1*:: RGEF-1b-GFP transgene restored CI values to near-WT levels in *rgef-1(−/−)* animals (Figs. 3E, 3F). Substantial, but incomplete rescue of chemotaxis was achieved with an *odr-3*::REGF-1b-GFP transgene. Partial restoration of chemotaxis may be due to lower transcriptional activity of *odr-3* relative to *odr-1* and *rgef-1* promoters. Although the *gpa-3* promoter enables RGEF-1b-GFP accumulation in multiple neurons, the *rgef-1* null phenotype persisted (Figs. 3E, 3F). I1, AWB and AWA neurons are not involved in BZ- or BU-induced chemotaxis. Thus, the results suggest that RGEF-1b GTP exchange activity in AWC sensory neurons is indispensable for activating neuronal circuitry underlying chemotaxis behavior. The observations establish a neuron-specific physiological role for a RasGRP.

Dominant negative RGEF-1b disrupts chemotaxis

Conserved Arg^{290} in the RGEF-1b catalytic domain was mutated to Ala (Park et al., 1994). RGEF-$1b^{R290A}$ protein accumulated in transfected cells, but did not promote loading of GTP onto LET-60 (Fig. 4A, lanes 3, 4). Cells expressing bombesin receptor were co-transfected with transgenes encoding WT RGEF-1b (0.2 μg DNA), Flag-LET-60 (1 μg DNA) and RGEF-$1b^{R290A}$ (plasmid DNA varied from 0–1 μg). In both bombesin-treated and unstimulated cells, LET-60-GTP content decreased as the ratio of RGEF-$1b^{R290A}$ cDNA:WT RGEF-1b cDNA increased (Fig. 4B, lanes 1–8). A 4-fold excess of RGEF-$1b^{R290A}$ transgene eliminated bombesin-induced GTP exchange activity of WT RGEF-1b (Fig. 4B, lanes 7, 8). Thus, RGEF-$1b^{R290A}$ is a dominant negative RasGRP.

Expression of RGEF-$1b^{R290A}$-GFP throughout the nervous system did not rescue chemotaxis in *rgef-1* null animals (Fig. 4C). Thus, RGEF-1b does not function as a scaffold in vivo; its GTP exchange activity is required for chemotaxis. Moreover, Arg^{290} was identified as an essential amino acid in the catalytic domain. Expression of RGEF-$1b^{R290A}$-GFP in the WT background suppressed chemotaxis to odorants detected by AWC neurons (Fig. 4D). The data show that RGEF-1b is essential for odorant-activated chemotaxis in a WT context.

RGEF-1b mediates chemotaxis by activating LET-60

By analogy with mammalian Ras and Rap1 mutants (Campbell et al., 2006), substitution of Gly^{12} with Val should ablate GTPase activity, thereby locking LET-60 or RAP-1 in an active, GTP-bound state (Fig. 5A). Replacement of Ser^{17} with Asn should generate dominant negative mutants of LET-60 and RAP-1. LET-60^{G12V} and RAP-1^{G12V} avidly bound GTP in unstimulated cells (Fig. 5B, lanes 1, 3). GTP loading was not increased by co-expression of RGEF-1b and addition of PMA (Fig. 5B, lanes 2, 4).

The *odr-1* promoter was used to direct LET-60^{G12V} synthesis in RGEF-1b depleted animals. Expression of LET-60^{G12V} in AWC neurons restored CI values for BZ and BU to ~ 75% of the WT level (Fig. 5C). In contrast, an *rgef-1*::RAP-1^{G12V} transgene did not rescue chemotaxis in *rgef-1(−/−)* animals (Fig. 5C). Expression of dominant negative LET-60^{S17N} in AWC neurons potently inhibited chemotaxis in WT animals (Fig. 5D). Synthesis of RAP-1^{S17N} in AWC neurons did not diminish chemotaxis (Fig. 5D). The results exclude RAP-1 as an RGEF-1b effector in AWC-dependent chemotaxis. Odorant-activated RGEF-1b promotes chemotaxis by switching on LET-60-mediated signal transduction in AWC neurons.

SOS-1, which activates LET-60 during development, does not compensate for impaired chemotaxis caused by RGEF-1b deficiency. However, SOS-1 could potentially cooperate with RGEF-1b to enhance odorant-induced signaling. Young adult animals carrying a temperature sensitive *sos-1*(*up604*) allele (Rocheleau et al., 2002) were incubated at the non-permissive temperature (25ºC) for 24 h to eliminate SOS-1 activity. SOS-1 depletion had no effect on chemotaxis (Fig. 5E).

LET-60 links odorant-activated RGEF-1b to MEK-2

To determine if ERK plays a prominent role in chemotaxis, we characterized effects of constitutively active and dominant negative MEK-2 on odorant-induced behavior. In *C. elegans*, LET-60, LIN-45 (RAF), MEK-2 and MPK-1 (ERK) constitute a unique Ras-ERK signal transduction pathway. MEK-2 phosphorylates and activates MPK-1, but has no effect other LET-60 effectors. LIN-45 activates MEK-2 by phosphorylating Ser^{223} and Ser^{227} in the MEK-2 activation loop (A-loop). Mutation of Ser^{223} and Ser^{227} to Glu^{223} and Asp^{227} generates constitutively active MEK-2; substitution of Ser^{223} and Ser^{227} with Ala creates a

dominant negative MEK-2 variant (Wu et al., 1995). Pan-neuronal and AWC-selective expression of MEK-2$^{S223A\ S227A}$-GFP (MEK-2-GFP(dn)) strongly inhibited chemotaxis in a WT background (Fig. 5F). Conversely, expression of the gain of function MEK-2$^{S223E\ S227D}$-GFP mutant (MEK-2-GFP(gf)) restored chemotaxis in *rgef-1(−/−)* animals (Fig. 5F).

AGE-1 (PI3K) is another effector of LET-60-GTP. However, chemotaxis was enhanced, not impaired, when AGE-1 activity was diminished by a partial loss of function mutation (*age-1(hx546)*) or depleted by incubating a temperature sensitive variant (*age-1(mg305)*) (Wang and Ruvkun, 2004) under non-permissive conditions (25ºC) for 24 h prior to assay (Fig. 5G). Thus, RGEF-1b links odorants to behavior principally by promoting MEK-2 activation in AWC neurons.

RGEF-1b mediates activation of MPK-1 by EGL-30 (Gαq), EGL-8 (PLCβ) and DAG

MEK-2 activates MPK-1 by phosphorylating Thr^{188} and Tyr^{190} in the MPK-1 A-loop. Dephosphorylation of either site suppresses MPK-1 catalytic activity. Thus, IgG directed against a di-phosphorylated A-loop peptide was used (with fluorophore-conjugated secondary antibody) to examine MPK-1 activation in vivo. Endogenous MPK-1 was inactive in the absence of stimuli (Fig. S4, A–C). Brief exposure to BZ elicited MPK-1 activation in AWC neurons (Fig. S4, D–F). Phospho-MPK-1 was evident in the cell body, as reported (Hirotsu et al., 2000). In contrast, BZ did not activate MPK-1 in *rgef-1(−/−)* animals (Fig. S4, J–L). Expression of an *odr-1*::RGEF-1b-GFP transgene restored BZ-induced MPK-1 phosphorylation in RGEF-1b deficient animals (Fig. S5, D–F). AWC-targeted expression of MEK-2$^{S223E\ S227D}$-GFP (MEK-2-GFP(gf)) promoted MPK-1 activation (*rgef-1(−/−)* background) in the absence or presence of BZ (Fig. S5, G–L). In contrast, synthesis of MEK-2-GFP(dn) in AWC abolished BZ-dependent MPK-1 activation in WT animals (Fig. 6, below). Thus, RGEF-1b and the LET-60-MEK-2 effector module couple an odorant stimulus to MPK-1 activation in AWC neurons.

MPK-1 phosphorylation in AWC neurons was quantified by measuring fluorescence signals emitted by immune complexes containing phospho-MPK-1, primary IgG and secondary IgG coupled to a DyLight 549 fluorophore. Fluorescence values for experiments described in Figs. S4 and S5 are given in Fig 6.

EGL-8, a PLCβ homolog, is activated by EGL-30 (Gαq) and generates DAG that mediates or modulates neuronal control of locomotion, food foraging, associative learning and other facets of *C. elegans* physiology. Thus, we determined whether EGL-30, EGL-8 and DAG control RGEF-1b in AWC neurons. Inactivating mutations in *egl-30* and *egl-8* cause movement defects that preclude chemotaxis assays. However, measurement of MPK-1 activity in AWC neurons enabled locomotion-independent analysis of putative RGEF-1b regulators.

BZ did not activate MPK-1 in an *egl-30(ad806)* lf mutant, whereas an *egl-30(ep271)* gf allele (Met^{244} to Ile) elicited persistent MPK-1 activity in untreated animals (Fig. 6). The Ile^{244} mutation increases effector binding affinity of EGL-30 (Fitzgerald et al., 2006). Incubation of *egl-30(ep271)* animals with BZ increased MPK-1 activity ~3-fold (Fig. 6). Robust MPK-1 activation probably reflects an additive effect of a BZ-induced increase in EGL-30^{M244I}-GTP content and higher effector affinity. RGEF-1b depletion abrogated odor-independent and BZ-induced MPK-1 phosphorylation in AWC neurons of an *egl-30(ep271), rgef-1(−/−)* double mutant (Fig. 6). The data show RGEF-1b mediates MPK-1 activation by EGL-30.

An *egl-8*(*n488*) null mutation prevented BZ-induced MPK-1 activation (Fig. 6). However, a DAG surrogate, PMA, bypassed the defect and activated MPK-1 in AWC neurons of EGL-8 deficient animals. In contrast, depletion of RGEF-1b eliminated PMA-triggered MPK-1 phosphorylation in AWC neurons (*rgef-1(−/−)* animals). Thus, like EGL-30, EGL-8 and PMA/DAG are upstream regulators of RGEF-1b in vivo.

High-affinity binding activity of the RGEF-1b C1 domain is essential in vivo

RGEF-1b-GFP was dispersed in the cytoplasm of unstimulated HEK293 cells (Fig. 7A, panels a and c). PMA and bombesin elicited translocation of RGEF-1b to a perinuclear location (Fig. 7A, panels b and d). The data suggest PMA and DAG enhance GTP exchange activity by recruiting RGEF-1b to internal membranes that contain transiently or persistently co-localized LET-60.

C1 domains are composed of ~50 amino acids and contain two His and six Cys residues that are conserved (Fig. 7B). Collectively, the Cys and His side chains ligate two zinc ions, thereby creating a rigid structure that supports a binding pocket. Three β strands and two hydrophobic loops (A and B) (Fig. 7B) generate surfaces that bind DAG/PMA and facilitate partial immersion of C1 domains into a lipid bilayer. A conserved Pro in loop A is critical for high-affinity PMA binding (Hurley and Misra, 2000). Consequently, Pro^{503} in RGEF-1b was mutated to Gly. The mutation extinguished basal GTP exchange (Fig. 7C, lanes 1, 3) and sharply suppressed GTP loading activity at a concentration of PMA (50 nM) that maximally activated WT RGEF-1b (Fig. 7C, lanes 2, 4; Fig. 7D lane 1, upper and lower panels). However, incubation of cells with high concentrations of PMA (200–400 nM) elicited similar, maximal catalytic activities for RGEF-$1b^{P503G}$ and RGEF-1b (Fig. 7D). The results indicate that the mutant exchanger folds normally, but Pro^{503} is essential for high-affinity PMA binding by the C1 domain.

RGEF-$1b^{P503G}$ failed to activate LET-60 when bombesin triggered DAG synthesis (Fig. 7C, lane 8). Bombesin peptide concentration (200 nM) was 20-fold higher than necessary to saturate bombesin receptors and optimally activate PLCβ (Feng et al., 2007). Thus, Pro^{503} is indispensable for coupling increased DAG content to RGEF-1b activation. Maximal, bombesin-induced production of DAG did not compensate for the diminished C1 domain function of RGEF-$1b^{P503G}$.

RGEF-$1b^{P503G}$ was not stably recruited to membranes by 50 nM PMA or 200 nM bombesin (Fig. 7A, panels f and h). Evidently, transient association of RGEF-$1b^{P503G}$ with membrane-bound, non-metabolized PMA was sufficient to modestly activate LET-60 (Fig. 7C, lane 4). Reduced binding affinity of RGEF-$1b^{P503G}$ for transiently-synthesized, rapidly-metabolized DAG prevented exchanger activation by endogenous second messenger (Fig. 7C, lane 8). Thus, high affinity DAG binding activity of the C1 domain is essential for intracellular targeting and maximal catalytic activity of RGEF-1b.

In vivo consequences of RasGRP C1 domain dysfunction are unknown. Therefore, animals expressing *rgef-1*::RGEF-1b or *rgef-1*::RGEF-$1b^{P503G}$ transgenes (*rgef-1(−/−)* background) were incubated with odorants detected by AWC or AWA neurons. RGEF-1b restored chemotaxis to both odorants (Fig. 7E). In contrast, pan-neuronal expression of RGEF-$1b^{P503G}$ did not alter low CI values observed in RGEF-1b deficient *C. elegans* (Fig. 7E). Thus, C1 domain-mediated targeting to membranes is a key determinant of a RasGRP function (chemotaxis) *in vivo*.

MPK-1 phosphorylation was assayed to determine if the RGEF-$1b^{P503G}$ mutation affected signaling in AWC neurons. Animals expressing *odr-1*::RGEF-1b or *odr-1*::RGEF-$1b^{P503G}$ transgenes (*rgef-1(−/−)* background) were treated with BZ. Expression of RGEF-1b-GFP

enabled robust, odorant-induced MPK-1 phosphorylation in AWC neurons (Fig. 6). In contrast, BZ-dependent MPK-1 activation was not detected in animals expressing RGEF-1b^{P503G}-GFP. AWC-selective expression of MEK-2-GFP(gf) elicited constitutive high level MPK-1 activation in both *egl-8* null and *rgef-1* null animals (Fig. 6). Thus, avid DAG binding by the RGEF-1b C1 domain is indispensable for odorant-induced activation of the LET-60-MEK-2 cascade and MPK-1 phosphorylation *in vivo.*

The C1 domain controls localization and catalytic activity of RGEF-1b

In PMA-treated cells, RGEF-1b-GFP co-localized with RFP-KDEL, a protein that accumulates in endoplasmic reticulum (ER) (Fig. S6, A–C). To elucidate the mechanism of activation, RGEF-1b and RGEF-1b^{P503G} were anchored at the cytoplasmic surface of ER by fusion with a targeting domain derived from cytochrome b5 (Bulbarelli et al., 2002) (Fig. S6F). ER-tethered RGEF-1b exhibited low activity in unstimulated cells (Fig. 7F, lane 1). However, GTP loading activity of tethered RGEF-1b increased markedly in cells incubated with 50 nM PMA (Fig. 7F, lane 2). In contrast, RGEF-1b^{P503G} was minimally activated by PMA, despite its association with ER (Fig. 7F lane 4). Thus, proper intracellular targeting is required, but not sufficient for RGEF-1b activation. High affinity binding activity of a bifunctional C1 domain is essential for ER targeting and inducing an RGEF-1b conformation that expresses maximal catalytic activity. The observations also indicate that RGEF-1b activates LET-60 at the ER.

Differential intra-neuronal targeting is required for RGEF-1b function

The effect of intracellular localization on RGEF-1b function was analyzed in vivo. Two AWC-targeted transgenes were expressed in *rgef-1(−/−)* animals (see Supplemental Experimental Procedures). The first encoded NT36-RGEF-1b-GFP, which contains amino acids 1–36 of ODR-3 (NT36) fused to the N terminus of RGEF-1b. NT36 targets proteins to the plasma membrane of cilium, dendrite and cell body. A second transgene encoded RGEF-1b-GFP-b5, in which *C. elegans* cytochrome b5 was fused to the C-terminus of RGEF-1b-GFP. A hydrophobic C-terminal domain anchors cytochrome b5 at the cytoplasmic surface of ER.

NT36-RGEF-1b-GFP accumulated in the AWC cell body, dendrite and cilium, but not the axon (Fig. S7C). The fusion protein did not alter the chemotaxis defect (Fig. S7, A, B). RGEF-1b-GFP-b5 accumulated in the AWC axon and cell body (Fig. S7F) and restored chemotaxis to BZ and BU (Fig. S7, D, E).

Inactivation of RGEF-1b EF hands does not impair odorant-induced chemotaxis

Neither a Ca^{2+} chelator (BAPTA-AM) nor inactivating mutations in EF hands impaired PMA-stimulated GTP exchange activity of RGEF-1b in transfected cells (Fig. S8). However, possibilities that Ca^{2+} binding by EF hand modules might affect stability, duration of activation or other properties of RGEF-1b were not excluded. Consequently, the physiological relevance of EF hand domains was evaluated in vivo.

EF-hand modules have a consensus motif, (D/E)X(D/E)X(D/E)GXIXX(D/E)(D/E). Asp (D) and Glu (E) carboxyl groups coordinate Ca^{2+}; Gly and Ile contribute structural features; and "X" represents any amino acid (Gifford et al., 2007). Mutations that eliminate negative charge from positions 1 and 12 in EF hands substantially decrease or eliminate Ca^{2+} binding affinity. Therefore, Asp^{1} and Glu^{12} were replaced in both RGEF-1b EF hands (see Fig. S1B). A quadruple mutant, named RGEF-1b(4A), was generated by substituting Asp^{432}, Glu^{443}, Asp^{461} and Glu^{472} with Ala. RGEF-1b deficient animals were reconstituted with *rgef-1*::RGEF-1b-GFP and *rgef-1*::RGEF-1b(4A)-GFP transgenes. Expression of either WT or mutant GEF restored chemotaxis to odorants to near-WT levels (Fig. 8A). Thus, defective

EF hand modules did not disrupt RGEF-1b mediated chemotaxis. The data imply that an increase in DAG is sufficient to enable (C1 domain-mediated) RGEF-1b activation, production of LET-60-GTP and downstream signaling in neurons *in vivo*. Ca^{2+} binding by RGEF-1b EF hands is dispensable for chemotaxis.

A conserved PKC phosphorylation site is not required for RGEF-1b mediated chemotaxis

DAG-activated PKCs increase RasGRP3 catalytic activity by phosphorylating Thr^{133} (Zheng et al., 2005). Amino acid sequences surrounding Thr^{133} in RasGRP3 and Ser^{135} in RGEF-1b are homologous. Moreover, RasGRP3 Thr^{133} and RGEF-1b Ser^{135} precede the catalytic domain by 18 amino acids and are embedded in a short linker region that couples REM to GEF domains in RasGRPs (Fig. S1, B and D). To determine if PMA elicits phosphorylation of Ser^{135} in situ, we prepared IgGs directed against an RGEF-1b peptide (amino acids 128–143, Fig. S1B) that contained phospho-Ser^{135}. Cells expressing HA-RGEF-1b were incubated with PMA or vehicle and GTP exchanger was precipitated from cell extracts with anti-HA IgGs. Phosphorylation of RGEF-1b Ser^{135} was minimal in unstimulated cells (Fig. 8B, upper panel, lane 3). However, Ser^{135} phosphorylation increased substantially when endogenous PKCs were activated by PMA (Fig. 8B, upper panel, lane 4). Specificity of the phosphopeptide-directed IgGs was verified by mutating Ser^{135} to Ala. RGEF-$1b^{S135A}$ was expressed and immunoprecipitated (Fig. 8B, lanes 5 and 6, lower panel). No signals were detected when the blot was probed with phosphorylation-site selective IgGs (Fig. 8B, upper panel, lanes 5 and 6). Thus, Ser^{135} in RGEF-1b is a target site for PMA-stimulated phosphorylation.

The relevance of Ser^{135} phosphorylation to RGEF-1b mediated chemotaxis was explored by reconstituting *rgef-1* null mutants with an *rgef-1*::RGEF-$1b^{S135A}$-GFP transgene. RGEF-$1b^{S135A}$-GFP rescued chemotaxis, yielding CI values for odorants that were similar to CIs obtained for WT *C. elegans* and null mutants expressing WT RGEF-1b-GFP (Fig. 8C). Thus, phosphorylation of Ser^{135} is not required for RGEF-1b mediated activation of the LET-60-MPK-1 pathway in neurons that control odorant-induced chemotaxis.

DISCUSSION

RasGRPs were discovered in studies on mammalian brain 12 years ago (Buday and Downward, 2008). They are expressed in neurons within several brain regions and their effectors regulate many facets of cell physiology (Bos et al., 2007; Toki et al., 2001). However, functions, regulation and effectors of neuronal RasGRPs are unknown. We have elucidated regulatory properties, a physiological function and effectors of RGEF-1b, a RasGRP homolog, in *C. elegans* sensory neurons. RGEF-1b has conserved catalytic, EF-hand and C1 domains that are hallmark features of RasGRPs. PMA and DAG recruit RGEF-1b from cytoplasm to membranes and stimulate its' catalytic activity. Both LET-60 and RAP-1 are RGEF-1b substrates. Thus, RGEF-1b is a new, but prototypical RasGRP.

The *rgef-1* gene promoter is active in neurons. Transcription was initiated just prior to hatching of L1 larvae. Promoter activity was sustained in all larval stages and adulthood. After hatching, *C. elegans* relies on extrinsic stimuli (food, ions, etc) to guide its behavior. The neuron-specific and temporal patterns of *rgef-1* gene expression suggest RGEF-1b could mediate behavioral responses to environmental stimuli throughout post-embryonic life.

Chemotaxis to volatile odorants was impaired in RGEF-1b deficient animals. Pan-neuronal or AWC-selective expression of RGEF-1b-GFP restored chemotaxis in *rgef-1* null animals. Conversely, pan-neuronal or AWC-selective expression of dominant negative RGEF-$1b^{R290A}$-GFP disrupted odorant-induced chemotaxis in WT animals. Thus, RGEF-1b

is indispensable for a fundamentally important *C. elegans* behavior. Odorant-induced chemotaxis enables acquisition of nutrients that optimize health and reproduction. The discovery that RGEF-1b mediates chemotaxis establishes a neuronal function for a RasGRP. The insight that expression of RGEF-1b in AWC neurons restores chemotaxis to attractive odorants illuminates the cellular basis for the *rgef-1* null phenotype. Signals disseminated by a DAG-activated RasGRP in AWC sensory neurons are essential for complex behavior of an intact animal.

RGEF-1b loads GTP onto LET-60 and RAP-1. Expression of constitutively active LET-60^{G12V} in AWC neurons restored chemotaxis to odorants in RGEF-1b deficient animals. Accumulation of dominant negative LET-60^{S17N} in AWC neurons (WT background) inhibited chemotaxis. Neither constitutively active nor dominant negative RAP-1 affected chemotaxis. Thus, RGEF-1b couples odorant stimuli to chemotaxis via LET-60-GTP.

The AGE-1-AKT-1 and LIN-45-MEK-2-MPK-1 signaling modules are effectors of LET-60-GTP (Han et al., 1993; Nanji et al., 2005). Elimination of AGE-1 activity from a temperature sensitive mutant and characterization of nematodes carrying a hypomorphic allele of *age-1* revealed that PI3K deficiency enhanced chemotaxis to BZ and BU. Thus, the LET-60-AGE-1-AKT-1 pathway is not required for attraction to odorants. Expression of constitutively active MEK-2-GFP(gf) restored AWC-dependent chemotaxis in the *rgef-1* null background. Conversely, synthesis of dominant negative MEK-2-GFP(dn) in AWC neurons of WT animals suppressed chemotaxis, thereby recapitulating the *rgef-1(−/−)* phenotype. The magnitude of effects elicited by MEK-2 mutants and the unique substrate specificity of MEK-2 suggested that RGEF-1b and LET-60 couple odorant stimuli to chemotaxis by triggering MPK-1 phosphorylation (activation).

BZ elicited MPK-1 phosphorylation in AWC neurons. RGEF-1b depletion or synthesis of MEK-2-GFP(dn) in WT AWC neurons abolished odorant-induced MPK-1 activation. Conversely, AWC-directed expression of RGEF-1b-GFP or MEK-2-GFP(gf) restored MPK-1 phosphorylation (and chemotaxis) in *rgef-1(−/−)* animals. Thus, RGEF-1b couples odorant stimuli to MPK-1 activation in AWC neurons by switching on the LET-60-MEK-2 signaling cascade. RGEF-1b mediated MPK-1 activation is a key step in transducing an odor stimulus into a behavioral response.

We characterized RGEF-1b regulators by determining how combinations of mutations, transgenes and stimuli affect MPK-1 phosphorylation in AWC neurons (Figs. 6, S4 and S5). The evidence placed RGEF-1b downstream from EGL-30 and its effector, EGL-8, and documented a prominent role of DAG in RGEF-1b activation in vivo. RGEF-1b is a key effector in a chemotaxis signaling pathway that includes EGL-30, EGL-8 and DAG as upstream activators. Identification of an EGL-30 coupled receptor (GPCR) that regulates EGL-8 activity and DAG production is a central goal for future studies.

In pioneering studies, Hirotsu et al showed that LET-60 mutations impair chemotaxis to IAA (Hirotsu et al., 2000). They proposed that a Ca^{2+}-regulated GEF activates neuronal LET-60 This idea was not substantiated and neither upstream regulators nor proximal LET-60 effectors were identified (Hirotsu et al., 2004). We discovered that DAG-regulated RGEF-1b activates LET-60 and MPK-1 in AWC neurons. When *C. elegans* encounters attractive odors, a pathway that includes EGL-30, EGL-8, DAG, RGEF-1b, LET-60, LIN-45, MEK-2 and MPK-1 transduces signals in AWC neurons that control behavior.

A chemotaxis defect in *rgef-1(−/−)* animals could be caused by diminished odorant detection, aberrant downstream signaling or altered NT release from AWC axons. A current model suggests that GPCRs, ODR-3 (a $G_{\alpha i/o}$-related protein), guanylate cyclases (ODR-1,

DAF-11), cGMP phosphodiesterase (cGMP PDE) and the cGMP-gated TAX-2/TAX-4 cation channel mediate signaling underlying odorant detection (Bargmann, 2006). Odorants, presumably bound by GPCRs in AWC cilia, elicit ODR-3 activation and a decline in AWC Ca^{2+} concentration (hyperpolarization) (Chalasani et al., 2007). A key, but unverified inference is that ODR-3 lowers cGMP by inhibiting ODR-1/DAF-11 and/or stimulating cGMP PDE, thereby closing cGMP-gated TAX-2/TAX-4 channels that mediate Ca^{2+} influx. Subsequent odorant dissociation triggers transient depolarization, which precedes restoration of tonic channel activity.

RGEF-1b deficient animals avoided BU or BZ after prolonged exposure to odorant in the absence of food. Since odorant detection is essential for the behavioral switch, the ODR-3-TAX-2/TAX-4 pathway is operative in AWC neurons lacking RGEF-1b. Characterization of *odr-3*, *tax-2* and *tax-4* mutants indicated that odorant-induced AWC hyperpolarization is a pre-requisite for MPK-1 activation by IAA (Hirotsu et al., 2000). Thus, the LET-60-MPK-1 pathway functions downstream from TAX-2/TAX-4 channels. The inability of odorants to activate MPK-1 in *tax-2* or *tax-4* mutants excludes the possibility that odorant receptor controls LET-60 activation via ODR-3.

Phosphorylated MPK-1 accumulated principally in the AWC cell body of IAA- and BZ-treated WT animals. Output from the LET-60-MPK-1 cascade evidently modulates an odorant-induced, ion-based signal at a site segregated from ciliary odor sensing machinery. A modulatory role explains why a combination of odorant and AWC-targeted expression of constitutively active LET-60 (or MEK-2) restores chemotaxis in *rgef-1(−/−)* animals.

PMA and DAG elicited translocation of RGEF-1b from cytoplasm to ER in HEK293 cells. Diminished DAG binding affinity of the RGEF-$1b^{P503G}$ C1 domain markedly decreased translocation, thereby segregating the GTP exchanger from LET-60. When RGEF-1b was anchored to ER by a Tb5 domain, only basal catalytic activity was observed. PMA (50 nM) robustly activated ER-tethered RGEF-1b, but only minimally stimulated ER-bound RGEF-$1b^{P503G}$. Thus, avid PMA/DAG binding by the C1 domain is crucial for (a) co-localizing RGEF-1b with LET-60 and (b) inducing or stabilizing a conformation of RGEF-1b that expresses high level catalytic activity. RGEF-1^{P503G} did not restore chemotaxis or MPK-1 phosphorylation to *rgef-1* null animals. Thus, C1 mediated targeting of RasGRP to membranes is a critical step in switching on the Ras/ERK pathway in vivo.

LET-60 is maximally homologous with K-Ras, which is farnesylated and often activated at the ER. Subsequently, K-Ras is routed to effector locations without passage through Golgi membranes (Karnoub and Weinberg, 2008). RasGRP-mediated activation of K-Ras (LET-60) at the ER may be a conserved mechanism for routing regulatory signals. LET-60-GTP could be guided to various ER-proximal locations by its membrane binding properties, affinities for effectors and association with specific transport vesicles.

Concentrating RGEF-1b (presumably at ER) in the AWC axon and cell body enabled MPK-1 activation and chemotaxis. Sequestration in non-axonal compartments evidently separated RGEF-1b from its substrate, thereby disrupting its function. RGEF-1b apparently exerts physiological effects at sites far removed from cilia. These observations and evidence for unimpaired odorant detection in *rgef-1* null animals, suggest the RGEF-1b-LET-60-MPK-1 pathway modulates olfactory signal transduction within AWC and/or synaptic transmission to interneurons.

Distinct DAG effectors modulate synaptic transmission in AWC and motor neurons. Odorant-induced hyperpolarization of AWC is accompanied by pre-synaptic, DAG-stimulated PKC-1 signaling activity that promotes chemotaxis (Tsunozaki et al., 2008). EGL-30 promotes NT release from motor neurons by stimulating EGL-8 (Lackner et al.,

1999). DAG activates UNC-13 (which facilitates synaptic vesicle docking and priming) and PKC-1, which promotes NP exocytosis (Sieburth et al., 2007). RGEF-1b may be a third DAG effector that modulates synaptic transmission. Elimination of a conserved PKC phosphorylation site did not alter the ability of RGEF-1b to mediate AWC-dependent chemotaxis. Thus, RGEF-1b is uncoupled from PKC-1 and promotes chemotaxis by a distinct pathway.

The idea that RasGRPs are regulated by Ca^{2+} is widely disseminated (Bos et al., 2007; Buday and Downward, 2008), but evidence is limited. RasGRPs 1 and 2 were weakly activated in ionomycin-treated cells, but RasGRP4 and a RasGRP2 splice variant were inhibited by increases in cytoplasmic Ca^{2+} (Clyde-Smith et al., 2000). To clarify this key tenet of RasGRP regulation, we introduced two severe loss of function mutations into both EF hands of RGEF-1b, thereby generating RGEF-1b(4A). The mutations slightly reduced basal, but not PMA-stimulated GTP exchange activity in transfected cells. Importantly, RGEF-1b(4A) fully restored odorant-induced chemotaxis in *rgef-1(−/−)* animals. Thus, disruption of Ca^{2+} binding activity had no effect on RGEF-1b function within neurons in vivo. In AWC neurons, DAG alone governs the ability of RGEF-1b to couple odorant-generated signals to activation of the LET-60-MPK-1 pathway and chemotaxis.

EXPERIMENTAL PROCEDURES

Transgene Expression in Cell Culture

HEK293 cells were grown and transfected with transgenes encoding WT or mutant RGEF-1b and either FLAG-LET-60 or FLAG-RAP-1, as previously described (Feng et al., 2007). Cells were co-transfected with bombesin receptor to observe effects of DAG on RGEF-1b activity. After serum-starvation (0.1% serum, 16 h), cells were stimulated by PMA or bombesin, which increased DAG. Cells were lysed on ice in 0.3 ml of Ral buffer (0.2 M NaCl, 50 mM Tris-HCl pH (7.4), 1% Triton X-100, 10% glycerol) containing protease inhibitors (Roche) and phosphatase inhibitors (Sigma). Lysates were clarified by centrifugation at 15,000 x g for 20 min at 4°C.

Western Immunoblot Assays

Detergent-soluble proteins were size-fractionated by electrophoresis in a denaturing polyacrylamide (10%) gel. Precision Plus Protein polypeptides (Bio-Rad) were used as molecular weight standards. Western blots of fractionated proteins were prepared and incubated with primary IgGs (1:1000) as previously reported (Ndubuka et al., 1993). Lanes in Western blots received 30 μg of protein. Antigen-antibody complexes were visualized and quantified by using peroxidase-coupled secondary IgGs in combination with chemiluminescence reagents and image analysis software (Image J and ImageQuant (GE Healthcare)). Signals were recorded on x-ray film. In some cases, secondary antibody tagged with Alexa Fluor 680 (Molecular Probes) was used and fluorescence signals were quantified in a Li-Cor Odyssey imaging system.

GTP Loading Assays

LET-60-GTP and RAP1-GTP were isolated from cell extracts by binding with immobilized, GST-tagged, RAS or RAP binding domains (GST-RBDs). A domain from RalGDS selectively binds RAP1-GTP; a domain from c-Raf binds Let-60-GTP (de Rooij and Bos, 1997; Franke et al., 1997). RAP-1-GDP and LET-60-GDP are not bound. GSH-Sepharose 4B beads (Pharmacia) containing 5 μg of bound GST-RalGDS-RBD or GST-Raf-RBD were added to clarified lysates. After incubation at 4°C for 3h, beads were isolated by centrifugation at 10,000 × g for 10 min. After 4 washes in Ral buffer, isolated proteins were analyzed by Western immunoblot assays.

Chemotaxis Assays

Assays were performed on 10 cm Petri plates (Bargmann and Horvitz, 1991). Attractant (1 μl) and 1 μl of ethanol (neutral control) were applied to the agar at opposite ends of the plate (0.5 cm from the edge). NaN_3 (1 mM) was added to attractant and ethanol to immobilize animals that reached the reservoirs. Animals (150) were placed at the center of the plate. After 2 h at 20°C, numbers of animals clustered at attractant (A) and ethanol (C) reservoirs were counted. A chemotaxis index (CI) was calculated: CI = (A − C)/(A + C + worms elsewhere). The maximum chemotaxis value is +1.0. CI values were measured on triplicate plates and averaged. Experiments performed with BZ, BU or IAA yielded similar results. Representative data, obtained using one, two or all three attractants, are presented.

Other Procedures

Characterization of RGEF-1a and RGEF-1b cDNAs; preparation of transgenes, expression vectors and transgenic animals; mutagenesis, DNA, protein and qR-PCR analyses; characterization of an *rgef-1* gene deletion; antibody production, intra-cellular targeting of RGEF-1b-GFP; immunofluorescence microscopy; and the MPK-1 activation assay are described in Supplemental Experimental Procedures.

Supplementary Material

Refer to Web version on PubMed Central for supplementary material.

Acknowledgments

This work was supported by NIH grants GM080615 (C. S. Rubin) and T32 HL007675 (L. Chen). We thank Erik Snapp, Dave Hall and Zeynep Altun for reagents, discussions and advice.

References

Bargmann, CI. WormBook, The C. elegans Research Community. Chemosensation in C. elegans. WormBook. 2006. http://www.wormbook.org

Bargmann CI, Hartwieg E, Horvitz HR. Odorant-selective genes and neurons mediate olfaction in C. elegans. Cell. 1993; 74:515–527. [PubMed: 8348618]

Bargmann CI, Horvitz HR. Chemosensory neurons with overlapping functions direct chemotaxis to multiple chemicals in C. elegans. Neuron. 1991; 7:729–742. [PubMed: 1660283]

Bos JL, Rehmann H, Wittinghofer A. GEFs and GAPs: critical elements in the control of small G proteins. Cell. 2007; 129:865–877. [PubMed: 17540168]

Buday L, Downward J. Many faces of Ras activation. Biochim Biophys Acta. 2008; 1786:178–187. [PubMed: 18541156]

Bulbarelli A, Sprocati T, Barberi M, Pedrazzini E, Borgese N. Trafficking of tail-anchored proteins: transport from the endoplasmic reticulum to the plasma membrane and sorting between surface domains in polarised epithelial cells. J Cell Sci. 2002; 115:1689–1702. [PubMed: 11950887]

Caloca MJ, Zugaza JL, Bustelo XR. Exchange factors of the RasGRP family mediate Ras activation in the Golgi. J Biol Chem. 2003; 278:33465–33473. [PubMed: 12782630]

Campbell PM, Singh A, Williams FJ, Frantz K, Ulku AS, Kelley GG, Der CJ. Genetic and pharmacologic dissection of Ras effector utilization in oncogenesis. Methods Enzymol. 2006; 407:195–217. [PubMed: 16757325]

Chalasani SH, Chronis N, Tsunozaki M, Gray JM, Ramot D, Goodman MB, Bargmann CI. Dissecting a circuit for olfactory behaviour in Caenorhabditis elegans. Nature. 2007; 450:63–70. [PubMed: 17972877]

Clyde-Smith J, Silins G, Gartside M, Grimmond S, Etheridge M, Apolloni A, Hayward N, Hancock JF. Characterization of RasGRP2, a plasma membrane-targeted, dual specificity Ras/Rap exchange factor. J Biol Chem. 2000; 275:32260–32267. [PubMed: 10918068]

Coughlin JJ, Stang SL, Dower NA, Stone JC. The role of RasGRPs in regulation of lymphocyte proliferation. Immunol Lett. 2006; 105:77–82. [PubMed: 16530850]

de Jong AP, Verhage M. Presynaptic signal transduction pathways that modulate synaptic transmission. Curr Opin Neurobiol. 2009; 19:245–253. [PubMed: 19559598]

de Rooij J, Bos JL. Minimal Ras-binding domain of Raf1 can be used as an activation-specific probe for Ras. Oncogene. 1997; 14:623–625. [PubMed: 9053862]

Feng H, Ren M, Chen L, Rubin CS. Properties, regulation, and in vivo functions of a novel protein kinase D: Caenorhabditis elegans DKF-2 links diacylglycerol second messenger to the regulation of stress responses and life span. J Biol Chem. 2007; 282:31273–31288. [PubMed: 17728253]

Fitzgerald K, Tertyshnikova S, Moore L, Bjerke L, Burley B, Cao J, Carroll P, Choy R, Doberstein S, Dubaquie Y, et al. Chemical genetics reveals an RGS/G-protein role in the action of a compound. PLoS Genet. 2006; 2:e57. [PubMed: 16683034]

Franke B, Akkerman JW, Bos JL. Rapid Ca2+-mediated activation of Rap1 in human platelets. EMBO J. 1997; 16:252–259. [PubMed: 9029146]

Gifford JL, Walsh MP, Vogel HJ. Structures and metal-ion-binding properties of the Ca2+-binding helix-loop-helix EF-hand motifs. Biochem J. 2007; 405:199–221. [PubMed: 17590154]

Han M, Golden A, Han Y, Sternberg PW. C. elegans lin-45 raf gene participates in let-60 ras-stimulated vulval differentiation. Nature. 1993; 363:133–140. [PubMed: 8483497]

Hirotsu T, Saeki S, Yamamoto M, Iino Y. The Ras-MAPK pathway is important for olfaction in Caenorhabditis elegans. Nature. 2000; 404:289–293. [PubMed: 10749212]

Hirotsu T, Saeki S, Yamamoto M, Iino Y. The Ras-MAPK pathway is important for olfaction in Caenorhabditis elegans (corrigenda). Nature. 2004; 432:653.

Hurley JH, Misra S. Signaling and subcellular targeting by membrane-binding domains. Annu Rev Biophys Biomol Struct. 2000; 29:49–79. [PubMed: 10940243]

Karnoub AE, Weinberg RA. Ras oncogenes: split personalities. Nat Rev Mol Cell Biol. 2008; 9:517–531. [PubMed: 18568040]

Krab LC, Goorden SM, Elgersma Y. Oncogenes on my mind: ERK and MTOR signaling in cognitive diseases. Trends Genet. 2008; 24:498–510. [PubMed: 18774199]

L'Etoile ND, Bargmann CI. Olfaction and odor discrimination are mediated by the C. elegans guanylyl cyclase ODR-1. Neuron. 2000; 25:575–586. [PubMed: 10774726]

Lackner MR, Nurrish SJ, Kaplan JM. Facilitation of synaptic transmission by EGL-30 Gqalpha and EGL-8 PLCbeta: DAG binding to UNC-13 is required to stimulate acetylcholine release. Neuron. 1999; 24:335–346. [PubMed: 10571228]

Lans H, Rademakers S, Jansen G. A network of stimulatory and inhibitory Galpha-subunits regulates olfaction in Caenorhabditis elegans. Genetics. 2004; 167:1677–1687. [PubMed: 15342507]

Nanji M, Hopper NA, Gems D. LET-60 RAS modulates effects of insulin/IGF-1 signaling on development and aging in Caenorhabditis elegans. Aging Cell. 2005; 4:235–245. [PubMed: 16164423]

Ndubuka C, Li Y, Rubin CS. Expression of a kinase anchor protein 75 depletes type II cAMP-dependent protein kinases from the cytoplasm and sequesters the kinases in a particulate pool. J Biol Chem. 1993; 268:7621–7624. [PubMed: 8463292]

Park W, Mosteller RD, Broek D. Amino acid residues in the CDC25 guanine nucleotide exchange factor critical for interaction with Ras. Mol Cell Biol. 1994; 14:8117–8122. [PubMed: 7969149]

Rocheleau CE, Howard RM, Goldman AP, Volk ML, Girard LJ, Sundaram MV. A lin-45 raf enhancer screen identifies eor-1, eor-2 and unusual alleles of Ras pathway genes in Caenorhabditis elegans. Genetics. 2002; 161:121–131. [PubMed: 12019228]

Sieburth D, Madison JM, Kaplan JM. PKC-1 regulates secretion of neuropeptides. Nat Neurosci. 2007; 10:49–57. [PubMed: 17128266]

Stone JC. Regulation of Ras in lymphocytes: get a GRP. Biochem Soc Trans. 2006; 34:858–861. [PubMed: 17052215]

Tazmini G, Beaulieu N, Woo A, Zahedi B, Goulding RE, Kay RJ. Membrane localization of RasGRP1 is controlled by an EF-hand, and by the GEF domain. Biochim Biophys Acta. 2009; 1793:447–461. [PubMed: 19168098]

Teixeira C, Stang SL, Zheng Y, Beswick NS, Stone JC. Integration of DAG signaling systems mediated by PKC-dependent phosphorylation of RasGRP3. Blood. 2003; 102:1414–1420. [PubMed: 12730099]

Thomas GM, Huganir RL. MAPK cascade signalling and synaptic plasticity. Nat Rev Neurosci. 2004; 5:173–183. [PubMed: 14976517]

Tian X, Gotoh T, Tsuji K, Lo EH, Huang S, Feig LA. Developmentally regulated role for Ras-GRFs in coupling NMDA glutamate receptors to Ras, Erk and CREB. EMBO J. 2004; 23:1567–1575. [PubMed: 15029245]

Tognon CE, Kirk HE, Passmore LA, Whitehead IP, Der CJ, Kay RJ. Regulation of RasGRP via a phorbol ester-responsive C1 domain. Mol Cell Biol. 1998; 18:6995–7008. [PubMed: 9819387]

Toki S, Kawasaki H, Tashiro N, Housman DE, Graybiel AM. Guanine nucleotide exchange factors CalDAG-GEFI and CalDAG-GEFII are colocalized in striatal projection neurons. J Comp Neurol. 2001; 437:398–407. [PubMed: 11503142]

Tsunozaki M, Chalasani SH, Bargmann CI. A behavioral switch: cGMP and PKC signaling in olfactory neurons reverses odor preference in C. elegans. Neuron. 2008; 59:959–971. [PubMed: 18817734]

Wang D, Ruvkun G. Regulation of Caenorhabditis elegans RNA interference by the daf-2 insulin stress and longevity signaling pathway. Cold Spring Harb Symp Quant Biol. 2004; 69:429–431. [PubMed: 16117677]

Wu Y, Han M, Guan KL. MEK-2, a Caenorhabditis elegans MAP kinase kinase, functions in Ras-mediated vulval induction and other developmental events. Genes Dev. 1995; 9:742–755. [PubMed: 7729690]

Zheng Y, Liu H, Coughlin J, Zheng J, Li L, Stone JC. Phosphorylation of RasGRP3 on threonine 133 provides a mechanistic link between PKC and Ras signaling systems in B cells. Blood. 2005; 105:3648–3654. [PubMed: 15657177]

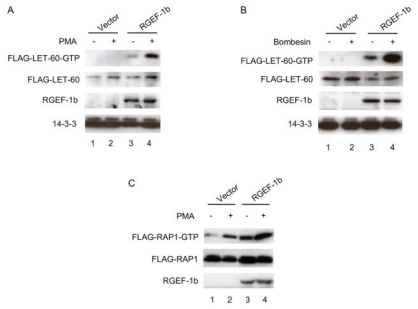

Figure 1. RGEF-1b loads GTP onto LET-60 and RAP-1

A,HEK293 cells were transfected with a FLAG-LET-60 transgene and either control plasmid (lanes 1 and 2) or plasmid encoding RGEF-1b (lanes 3 and 4). After incubation with vehicle or 50 nM PMA for 15 min, cells were lysed and LET-60-GTP was precipitated from samples containing 300 μg of protein (Experimental Procedures). Precipitated proteins and samples of total detergent soluble protein (30 μg/lane) were assayed by Western immunoblot analysis. LET-60-GTP and total LET-60 were detected by probing blots with anti-Flag IgGs. RGEF-1b was detected with anti-RGEF-1b IgGs. Incubation with secondary IgGs, and recording and quantification of chemiluminescence signals were performed as described in Experimental Procedures. Chemiluminescence signals, recorded on x-ray film, are shown. ***B***, cells were co-transfected with FLAG-LET-60 and bombesin receptor transgenes and either control vector or expression plasmid encoding RGEF-1b. Cells were incubated with vehicle or 200 nM bombesin (10 min) before lysis. Samples were processed as described in ***A. C***, cells were co-transfected a FLAG-RAP-1 transgene and either empty vector or RGEF-1b transgene. Assays were performed as described in ***A***. Similar results were obtained in 3 experiments.

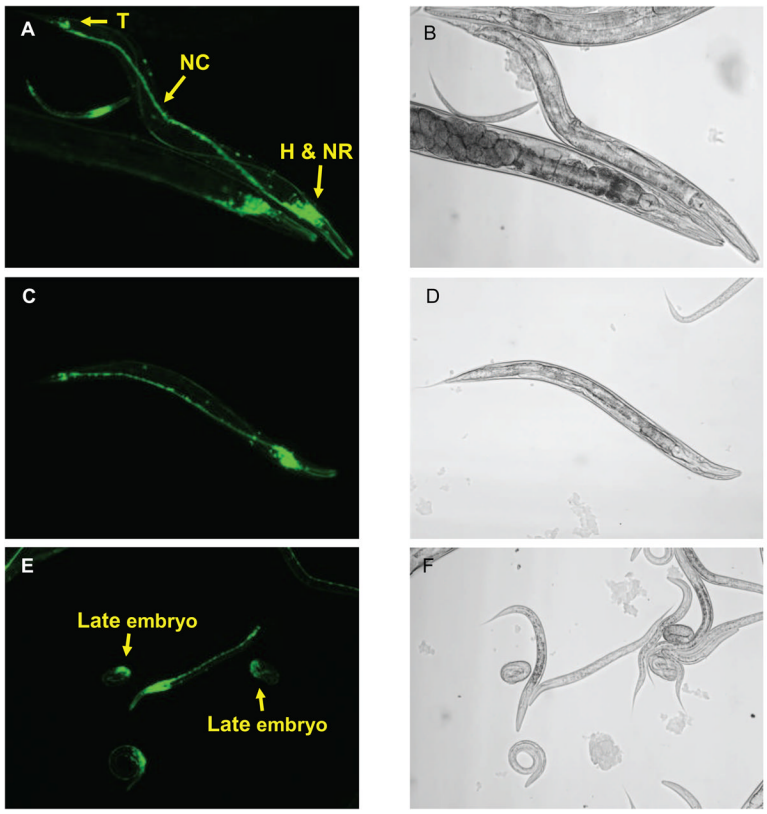

Figure 2. The *rgef-1* promoter is active in neurons

An *rgef-1*::GFP transgene was expressed in *C. elegans*. Accumulation of GFP was monitored by fluorescence microscopy. ***A, C*** and ***E*** show GFP fluorescence; ***B, D*** and ***F*** are corresponding phase micrographs. ***A*** and ***C*** show the *rgef-1* promoter is active throughout the nervous system. GFP is evident in head neurons (H), nerve ring (NR), tail neurons (T) and nerve cord (NC). ***E***, *rgef-1* promoter activity is initially observed in late embryos.

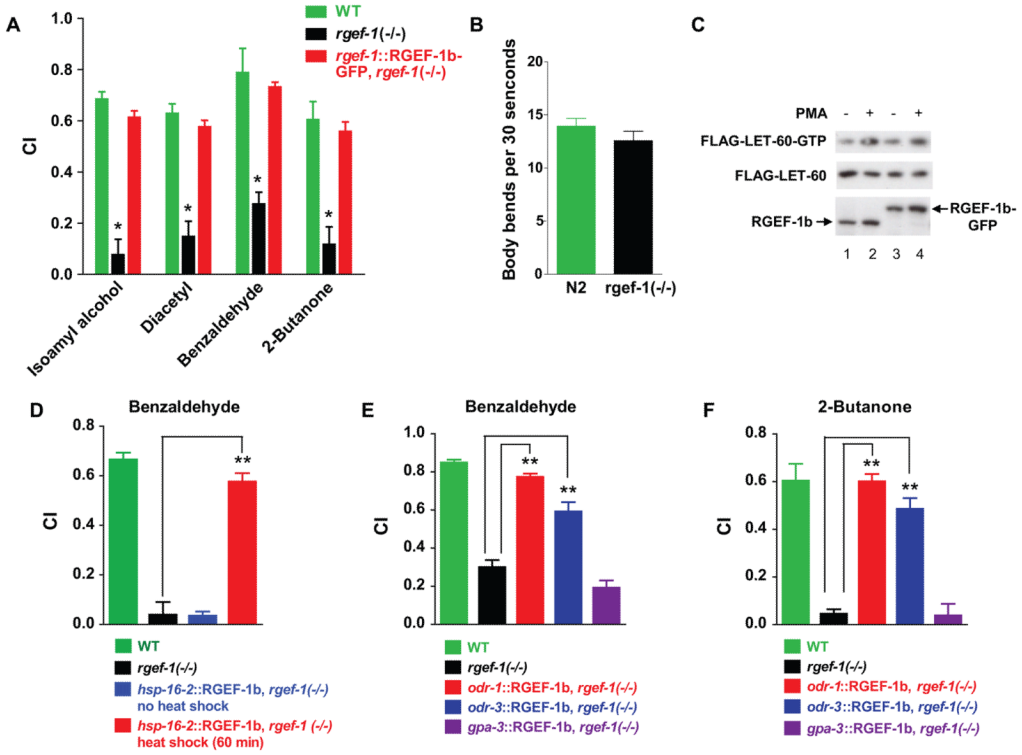

Figure 3. RGEF-1b is essential for chemotaxis to volatile odorants

A,WT, *rgef-1(−/−)* animals and animals expressing an *rgef-1*::RGEF-1b-GFP transgene (*rgef-1(−/−)* background) were assayed for chemotaxis. Chemotaxis index (CI) values are plotted; error bars are SEM. **P*< 0.0005 compared with WT animals, Dunnett's *t* test. ***B,*** WT or *rgef-1(−/−)* animals were assayed for locomotion on a bacterial lawn. The number of body bends in a 30 s time interval was determined for 20 WT or rgef-*1(−/−)* animals. Mean values and SEM are shown. ***C***, HEK293 cells were transfected with transgenes encoding FLAG-LET-60 and either RGEF-1b (lanes 1, 2) or RGEF-1b-GFP (lanes 3, 4). Cells were incubated with vehicle or PMA and assayed for LET-60-GTP, LET-60 and RGEF-1b content by immunoblotting. ***D***, an *hsp-16.2*::RGEF-1b transgene was inserted into *rgef-1(−/−)* animals. WT, *rgef-1(−/−)* and transgenic *C. elegans* were grown to the young adult stage at 20ºC. Control transgenic animals were maintained at 20ºC. Others were incubated at 32ºC for 60 min and returned to 20ºC for 2 h to enable recovery from heat stress. Subsequently, animals were assayed for chemotaxis to BZ. ***E*** and ***F,*** WT *C. elegans*, *rgef-1(−/−)* animals and animals expressing RGEF-1b-GFP under regulation of *odr-1*, *odr-3* or *gpa-3* promoters (*rgef-1(−/−)* background) were assayed for chemotaxis. Assays ***D–F*** were performed in triplicate; error bars are SEM. ***P*< 0.0001 compared with *rgef-1* null animals, Bonferroni's *t* test. Similar results were obtained in 3 experiments.

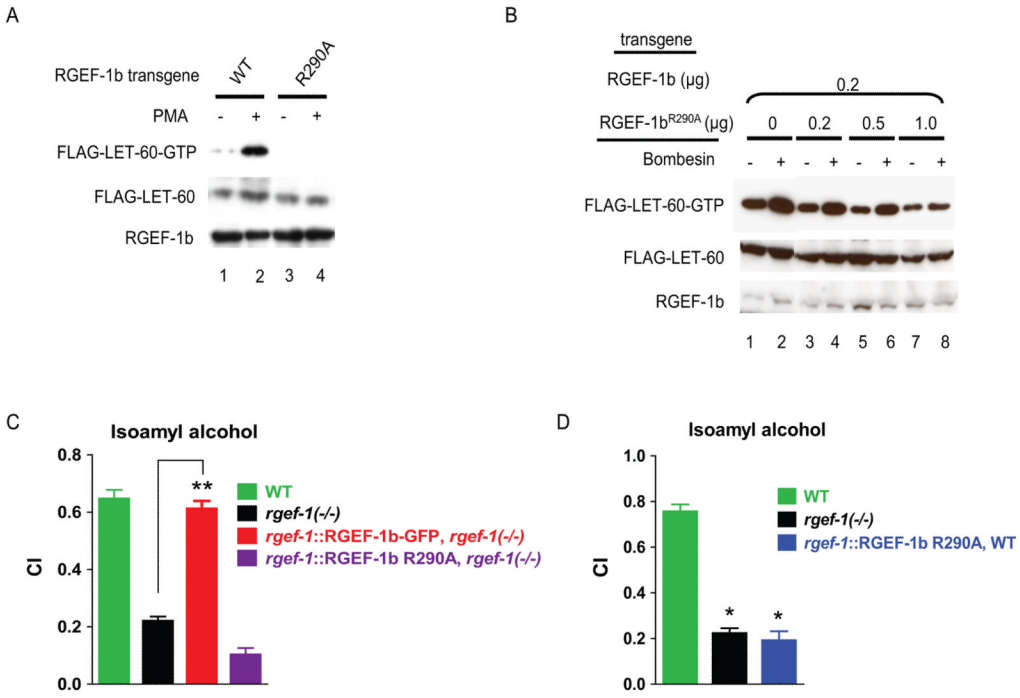

Figure 4. Mutation of Arg^{290} to Ala suppresses RGEF-1b activity and odorant-induced chemotaxis

A,cells were transfected with transgenes encoding FLAG-LET-60 and either RGEF-1b (lanes 1, 2) or RGEF-1b^{R290A} (lanes 3, 4). Cells were incubated with vehicle or PMA and assayed for LET-60-GTP, LET-60 and RGEF-1b content by immunoblotting. ***B***, cells were co-transfected with plasmids encoding bombesin receptor (0.1 μg DNA), WT RGEF-1b (0.2 μg DNA), FLAG-LET-60 (1 μg DNA) and RGEF-1b^{R290A} (DNA varied). Cells incubated with 200 nM bombesin (10 min) and untreated cells were assayed for LET-60-GTP content. ***C*** and **D**, indicated *C. elegans* strains were assayed for chemotaxis to IAA. Error bars are SEM. ***P*< 0.0001 compared with *rgef-1(−/−)* animals, Bonferroni's *t* test; *P< 0.0001 compared with WT, Dunnett's *t* test. Similar results were obtained in 3 experiments.

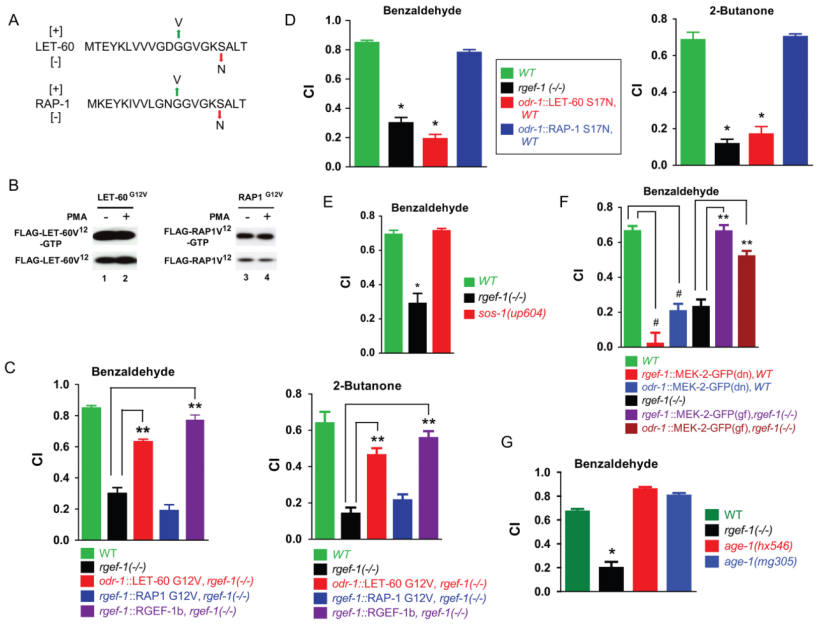

Figure 5. RGEF-1b couples odorants to chemotaxis by activating of LET-60 and MEK-2

A, N terminal amino acid sequences of LET-60 and RAP-1. Mutation of Gly^{12} to Val and Ser^{17} to Asn create constitutively active and dominant negative variants, respectively. ***B***, cells were co-transfected with plasmids encoding RGEF-1b and either FLAG-LET-60^{G12V} or FLAG-RAP-1^{G12V}. Cells were incubated with 50 nM PMA as indicated and assayed for LET-60-GTP or RAP-1-GTP content. ***C, D, E, F*** and ***G***, chemotaxis assays were performed on the indicated strains. In ***E* and *G***, animals were incubated at 25ºC for 24 h prior to assays to incapacitate temperature sensitive variants of SOS-1 and AGE-1, respectively. Error bars are SEM. **P*< 0.001 compared to WT *C. elegans*, Dunnett's *t* test; ***P*< 0.001 compared to *rgef-1(−/−)* animals, Bonferroni's *t* test; # *P*<0.001 compared to WT animals, Bonferroni's *t* test. Similar results were obtained in 3 experiments.

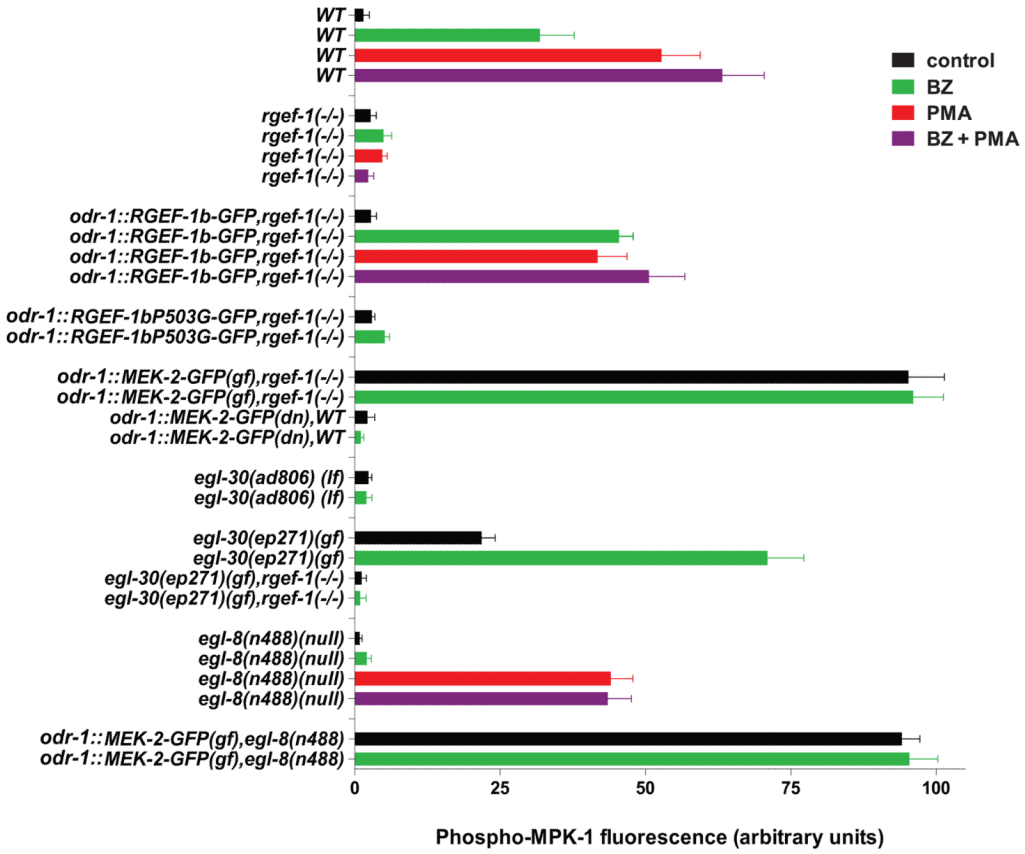

Figure 6. RGEF-1b mediates activation of MPK-1 by odorant, EGL-30, EGL-8 and DAG

Specified animals were incubated with buffer (control) or buffer containing BZ (1:10,000 dilution), PMA (300 nM) or BZ plus PMA for 3 min at 21°C, prior to fixation and permeabilization. Endogenous phospho-MPK-1 in AWC neurons was visualized by immunostaining (Supplemental Experimental Procedures). Fluorescence signals proportional to the abundance of di-phosphorylated (activated) MPK-1 in AWC neurons were recorded from 15 animals for each experimental condition and quantified. Mean values are presented; error bars are SEM. Similar results were obtained in 3 experiments.

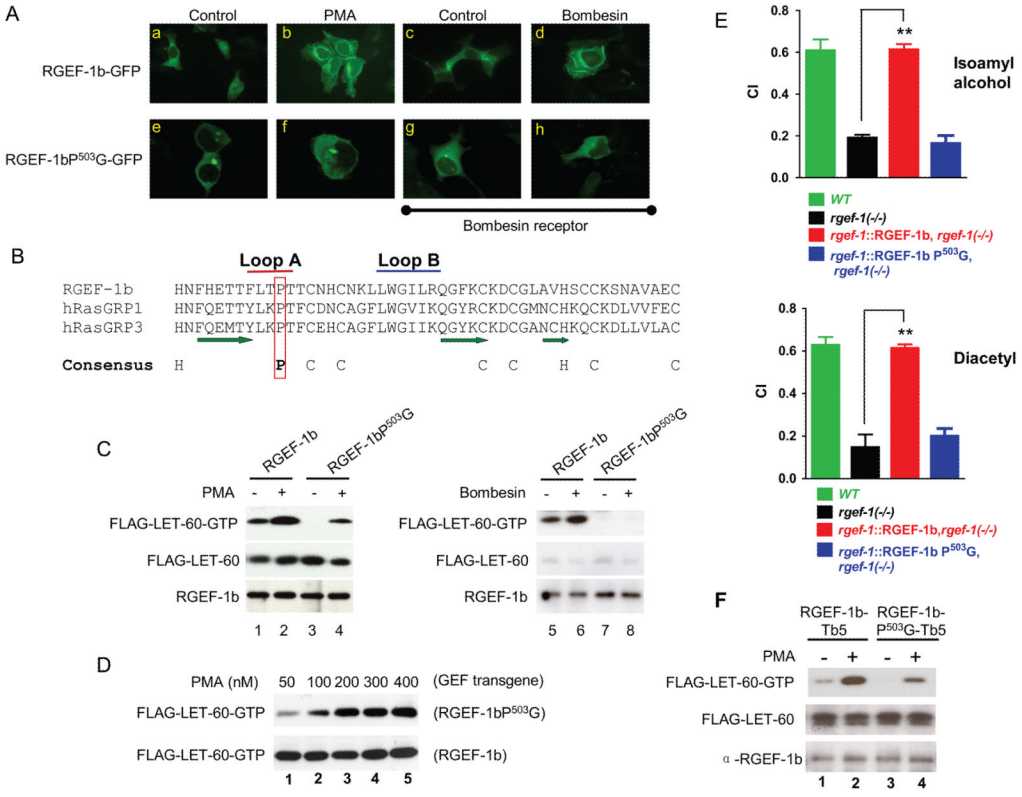

Figure 7. A C1 domain mediates RGEF-1b translocation and activation; loss of C1 function disrupts chemotaxis

A, cells were transfected with RGEF-1b-GFP, RGEF-1b^{P503G}-GFP and bombesin receptor transgenes as indicated. After incubation with vehicle, 50 nM PMA (10 min) or 200 nM bombesin (5 min), cells were fixed and GFP fluorescence was recorded via microscopy. ***B,*** amino acid sequences of C1 domains from RGEF-1b and RasGRPs 1 and 3 are aligned. Amino acids that generate A and B loops of the binding pocket are indicated by red and blue bars, respectively. β strands are marked by green arrows. A Pro residue predicted to mediate high affinity binding of PMA and DAG is enclosed in a red rectangle. Positions of conserved Cys (C) and His (H) residues are shown below the sequences. ***C***, cells were co-transfected with transgenes encoding FLAG-LET-60 and either RGEF-1b or RGEF-1b^{P503G}. Some cells also expressed bombesin receptor (lanes 5–8). Cells were incubated with 50 nM PMA or 200 nM bombesin and assayed for LET-60-GTP, LET-60 and RGEF-1b content by immunoblotting. ***D***, cells were co-transfected with transgenes encoding FLAG-LET-60 and either RGEF-1b^{P503G} or WT RGEF-1b. Cells were incubated with indicated amounts of PMA (10 min) and assayed for LET-60-GTP content by immunoblotting. ***E***, indicated animals were assayed for chemotaxis using odorants detected by AWC (IAA) and AWA (diacetyl) neurons. Error bars are SEM. $^{**}P < 0.001$ compared to *rgef-1(−/−)* animals, Bonferroni's *t* test. **F**, cells were co-transfected with transgenes encoding FLAG-LET-60 and either RGEF-1b-Tb5 or RGEF-1b^{P503G}-Tb5. "Tb5" is a C-terminal, ER targeting domain that was appended to WT and mutant GEFs. Cells were incubated with PMA and assayed for LET-60-GTP content as described above.

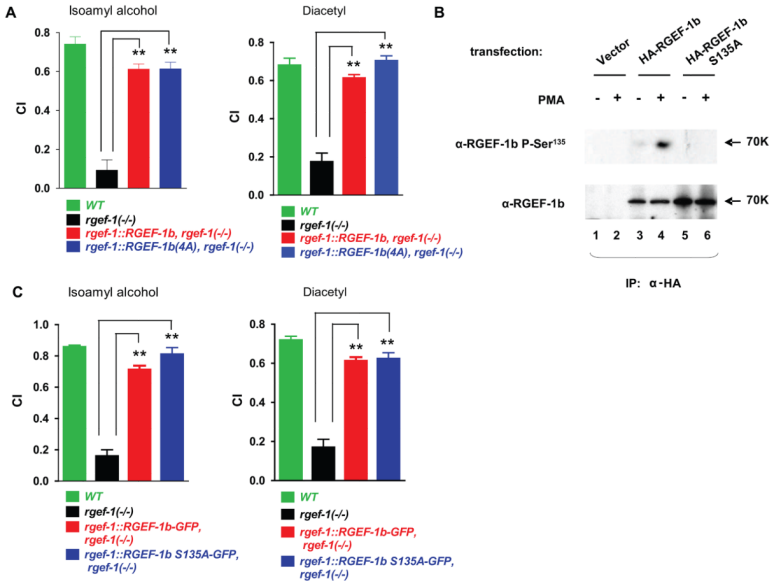

Figure 8. Ca^{2+} binding by EF hands and a PKC phosphorylation site are dispensable for RGEF-1b mediated chemotaxis

A, specified *C. elegans* strains were tested for chemotaxis to odorants detected by AWC (IAA) and AWA (diacetyl) neurons. ***B,*** HEK293 cells were transfected with empty vector or an HA-RGEF-1b or HA-RGEF-$1b^{S135A}$ transgene. Cells were incubated with 50 nM PMA (15 min) as indicated, prior to lysis. Anti-HA IgGs (1.5 μg) were added to aliquots of detergent-soluble proteins (300 μg). Antigen-antibody complexes were analyzed by Western immunoblot assays. Blots were probed with IgGs directed against P-Ser^{135}-RGEF-1b (*upper panel*) or a non-phosphorylated RGEF-1b epitope (*lower panel*). ***C,*** the indicated *C. elegans* strains were assayed for chemotaxis. Error bars are SEM. $^{**}P < 0.001$ compared to *rgef-1(−/−)* animals, Bonferroni's *t* test. Similar results were obtained in 3 experiments.